Author Manuscript

Author Manuscript

Author Manuscript

Author Manuscript

HHS Public Access

Author manuscript

Neuromethods. Author manuscript; available in PMC 2019 May 30.

Published in final edited form as:

Neuromethods. 2018 ; 134: 39–71. doi:10.1007/978-1-4939-7549-5_3.

Single-Unit Extracellular Recording from the Cerebellum During Eyeblink Conditioning in Head-Fixed Mice

Shane A. Heiney, **Shogo Ohmae**, **Olivia A. Kim**, and **Javier F. Medina**

Abstract

This chapter presents a method for performing in vivo single-unit extracellular recordings and optogenetics during an associative, cerebellum-dependent learning task in head-fixed mice. The method uses a cylindrical treadmill system that reduces stress in the mice by allowing them to walk freely, yet it provides enough stability to maintain single-unit isolation of neurons for tens of

---

Note 1. Treadmill

Note 2.1. Make sure to measure the light transmission through your fibers using the patch fiber that you intend to use during your experiment, as differences in the patch fiber connectorization quality will affect light transmission.

Note 2.2. You can measure light transmission both before and after an experiment, even if the optical fiber has been chronically implanted. If the fiber has been chronically implanted, carefully extract the fiber from the brain after euthanizing your animal. Soak the extracted implant in 70% EtOH for a few hours to disinfect it. You may also rinse the extracted implant a few times in distilled water. After you have allowed the implant to dry, you can then measure the degree of light transmission through it as you did before implantation. This will allow you to know whether the fiber may have been damaged during your experiment.

Note 3.1. In addition to the advice given in *Thorlabs Guide to Connectorization and Polishing of Optical Fibers*, it can be helpful to use a pin vise to protect the fibers while polishing.

Note 3.2. It is a good idea to perform the most difficult fiber construction steps as early as possible while making each fiber. This way, you will waste less time building fibers that you ultimately break.

Note 3.3. Instead of cleaving the fibers by taping them to a desk and manually scoring them, you can use Thorlabs posts and an RA90 to support a micromanipulator. Then, hold a fiber and ferrule in the micromanipulator's electrode holder using a pin vice. Use another RA90 to hold a ruby scribe at a right angle to the fiber. You can then use the micromanipulator to carefully score the fiber for more precise cleaving.

Note 4. Surgery

Note 5. Eyeblink Conditioning

Note 6.1. Tungsten electrodes are standard for a wide variety of purposes. These electrodes can be manufactured with thin out-side diameters (e.g., 80 μm; FHC) and are rigid enough that they can penetrate the dura and remain straight even after many recording sessions. These electrodes can also be used to make electrolytic lesions at recording sites.

Note 6.2. Platinum/iridium (Pt/Ir) electrodes are not as rigid as tungsten for a given diameter, but they don't get damaged as much as tungsten by electrical stimulation or electrolytic lesioning, so they can be used longer. They are also available for purchase in thin outside diameters (e.g., 80 μm; Alpha-Omega).

Note 6.3. Pulled glass electrodes are useful for marking recording sites by dye injection (e.g. 2% pontamine sky blue in 3 M potassium acetate). These electrodes can also be constructed to have small tip sizes (tip size = 2 μm, around 5 MOhm), allowing for large signal-to-noise ratio recordings of single Purkinje cells and excellent resolution of the calcium waves of the complex spike. Alternately, glass electrodes can be constructed to have larger tip sizes (tip size = 5–8 μm, around 2 MOhm), which makes it easier to locate Purkinje cells.

Note 6.4. Electrodes with larger tip sizes (impedance <1.0 MOhm) are ideal for recording climbing fiber local field potentials. The impedance of electrodes used for recording simple and complex spikes from Purkinje cells or action potentials from the deep cerebellar nuclei is somewhat a matter of personal preference. Larger tip sizes (lower impedance) allow the experimenter to detect electrical activity from further away but can make it more difficult to achieve single-unit instead of multiunit isolation. Smaller tip sizes (higher impedance) allow the experimenter to more easily isolate single-units, but it can be difficult to find cells using these electrodes.

Note 6.5. For microstimulation and electrolytic lesioning, be sure to select an electrode that can pass the desired current. Use Ohm's law to determine the maximum electrode resistance (impedance) that can be used given the supply voltage of your stimulus isolation unit and the desired current.

Author Manuscript Author Manuscript Author Manuscript Author Manuscript

minutes to hours. Using this system, we have investigated sensorimotor coding in the cerebellum while mice perform learned skilled movements.

Keywords

Cerebellum; Classical conditioning; Electrophysiology; Behavior; Motor learning

1 Introduction

Single-unit extracellular recordings have a rich history of use for the investigation of neural coding during behavior in many animal models [1]. Despite exciting advances in multi-neuron recording technologies such as tetrodes and silicon linear or matrix arrays, single-unit recording with metal or glass electrodes is still the gold standard for interrogating neural spiking, especially in deep brain areas with densely packed cells such as the cerebellum. The method allows the investigator to relate the spiking of individual neurons to sensory events and behavior, and thus allows one to examine the “neural code” with unparalleled fidelity.

Despite its advantages, single-unit extracellular recording in the cerebellum has only recently begun to be used in experiments on awake, behaving mice [2–7]. Unlike other model species, the restraint required for stable, acute single-unit recordings in the cerebellum typically elicits a stress response in mice, which can prevent effective task performance or engage fear-related circuits that mask or interfere with the behavior under study [8–10]. However, we have found that mice tolerate head restraint when permitted to walk freely on a treadmill. The ability to walk at will reduces stress and allows the mice to learn and perform a cerebellum-dependent associative motor learning task [11, 12]. Head fixation allows the investigator to exert fine control over stimulus presentation, collect high-quality extracellular single-unit recordings, and precisely measure behavior. Thus, the treadmill system facilitates the collection of datasets that can be used to correlate neural activity with stimulus presentation and behavior. When used in combination with techniques such as optogenetics or pharmacology [7, 12], the system also permits investigators to test the causal relationships between neural activity and behavior.

While it can be used in many different tasks, we use the head-fixed treadmill system for an associative motor learning task called eyeblink conditioning (EBC). During EBC, the animal is presented with repeated trials in which a neutral stimulus like a flash of light (conditioned stimulus, CS) precedes a blink-eliciting air puff to the cornea (unconditioned stimulus, US) [13, 14]. After many pairings of light and puff presentation, the animal learns to blink (conditioned response, CR) when it sees the light, such that the eye is closed by the time the puff arrives. EBC in mice requires an intact cerebellum [12, 15], and work in other animal species indicates that the memory for the association is formed and maintained within cerebellar circuits [16, 17]. Further, studies in mutant mice have identified specific cerebellar plasticity mechanisms that are required for EBC [15, 18–20]. Thus, EBC is an excellent model behavior for studying cerebellar mechanisms of learning and memory.

This chapter will present methods we have developed that specifically allow for the recording and optogenetic manipulation of multiple cell types within the cerebellar circuit

Author Manuscript Author Manuscript Author Manuscript Author Manuscript

during EBC, including Purkinje cells (PCs) and deep cerebellar nuclei (DCN) cells. However, many aspects of the described techniques should be useful for anyone wishing to make extracellular single-unit recordings in awake, behaving mice.

2 Materials

The apparatus we use for EBC and in vivo electrophysiology consists of mostly off-the-shelf components and a few custom parts and software. Below we describe the materials needed to assemble an apparatus like ours and give some assembly instructions. We also provide a list of materials required for the surgeries needed to prepare mice for these experiments. The heart of the EBC system is a cylindrical treadmill and infrared-sensitive high-speed camera that are mounted on an optical breadboard. Various components for stimulus delivery and electrophysiological recording are then mounted around the treadmill and camera systems, as depicted in Fig. 1.

2.1 General Materials

- Vibration isolation table (Newport; VIS3030-PG2–325A)

2.2 Treadmill System

Materials

- Two ½” diameter posts (12” length) (Thorlabs TR12)
- Two right-angle mounts for ½” diameter rods (Thorlabs RA90)
- Two ½” diameter brass or steel rods (6” length) (custom machined for holding headplate; schematic available at http://github.com/blinklab) (Fig. 1f)
- Two 2–56 screws for attaching headplate to brass rods
- One textured foam cylinder 6” diameter (Amazon (Exervo) TeraNova) (Fig. 1k)
- One ¼” diameter aluminum rod at least 3” longer than the cylinder (McMaster-Carr 9061K33)
- Two low-friction ball bearings (McMaster-Carr 3759T37)
- One bearing mount (custom machined from aluminum or 3D printed; schematic available at http://github.com/blinklab)
- One bearing and rotary encoder mount (custom machined from aluminum or 3D printed, schematic available at http://github.com/blinklab) (optional: use a second bearing mount if not using an encoder)
- One rotary encoder compatible with a ¼” diameter rod (e.g., Karlsson Robotics E6C2-CWZ3E 1024 count/revolution quadrature encoder) (optional) (Fig. 1l)
- One tube for connecting axle and rotary encoder (optional)

Author Manuscript Author Manuscript Author Manuscript Author Manuscript

Construction

1. Cut the foam cylinder to 4–6” long, and drill a hole through the middle of the cylinder that is slightly less than ¼” diameter so that the ¼” rod can fit snugly. Take care not to deform the cylinder, and be certain that the hole runs directly through the center of the cylinder (*see* Note 1.1).
2. Cut the ¼” diameter aluminum rod to be 3–4” longer than your foam wheel. Insert the rod into the hole that you drilled.
3. Gently press the bearings into the custom aluminum mounts (*see* Note 1.2).
4. If using a rotary encoder, attach the rotary encoder to the aluminum encoder mount. Cut a ½” length of tubing and slide it onto the axle of the rotary encoder. If not using a rotary encoder, use a second custom bearing mount in place of the encoder mount.
5. Insert each end of the axle into one of the bearings. Make sure that one end of the axle nearly makes contact with the rotary encoder. Slide the tubing from the encoder partially onto the axle so that the axle and rotary encoder spin together. Set the treadmill, encoder, and mount aside.
6. Screw two 12” posts into about the center of your vibration isolation table or breadboard so that the posts can accommodate the treadmill and mounts. Make sure that the posts are screwed very tightly into the breadboard.
7. Slide the mounts/treadmill onto the ½” posts so that the treadmill can spin freely. The wheel is spinning freely enough if it rocks back and forth after a test spin.
8. Place one right-angle mount on each post, about 1 ½” above the surface of the treadmill, so that the headplate bars can be passed through the mounts and meet above the treadmill. Adjust the right-angle mounts until the headplate bars can hold a headplate without straining the metal. Rotate the headplate bars so that they are at a known angle relative to the surface of the vibration isolation table. Also make sure that this angle will hold the mouse’s head in a reasonable position.

Maintenance

1. Thoroughly clean the surface of the wheel with 70% EtOH or a laboratory cleaner of your choice ASAP after removing the mouse from the wheel. This will help prevent too much urine from soaking into the foam.
2. Clean the area around the foam wheel. Urine and feces are sprayed off of the wheel when the mouse runs. It can be helpful to lay a paper towel or other disposable materials underneath the wheel to collect the majority of the mouse’s waste.

Note 1.1. Make the cylinders as perfectly as possible. If the axle is not centered in the foam, the treadmill will wobble when rotated, which can reduce recording stability and stress the mouse.

Note 1.2. Do not force the bearings into the mounts, as this will deform them and make it more difficult for the mouse to move the treadmill.

Author Manuscript Author Manuscript Author Manuscript Author Manuscript

3. When you apply cleaner to the wheel, moisten the paper towel or other disposable wipes away from the wheel. Doing other-wise can cause the cleaning solution to splatter on the equipment around the wheel.

2.3 Camera System

Materials

- One high-speed camera (e.g., Allied Vision Technologies GE680 gigabit Ethernet camera) (Fig. 1c)
- One lens for camera (Tamron TAM-23FM25-L)
- One extension tube for lens (1st Vision LE-EX-10 or LE-EX-5)
- One Ethernet card with support for jumbo packets (if using gigabit camera) (e.g., Intel PRO/1000 GT PCI)
- One Cat6 Ethernet cable (if using gigabit camera)
- One IR light source and power supply (Bosch EX12LED or similar) (Fig. 1d)
- One ½” diameter post (12” length) (Thorlabs TR12)
- Two knuckle joint (Panavise 851–00)
- One adapter to couple the knuckle joint and high-speed camera (custom-made, aluminum)
- One ½” diameter post (2–4” length) (Thorlabs TR2-TR4)
- Two right-angle mounts for ½” diameter posts (Thorlabs RA90)
- One BNC to SMB cable for triggering camera from data acquisition system (Fairview Microwave FMC0816315–72 is compatible with GE680)

Setup

1. Install high-speed camera drivers and software according to manufacturer instructions.
2. Attach the camera to a 2–4” long ½” diameter post using the knuckle joint and the custom camera mount.
3. Slide the 2–4” long post into one of the right-angle mounts.
4. Screw a 12” long ½” diameter post into the breadboard.
5. Slide the right-angle mount connected to the post and camera onto the 12” post. Check that the camera can be positioned roughly to point toward the future location of the mouse’s face. If not, repeat until you get a good approximate location.
6. Attach the infrared light to a knuckle joint, and attach the knuckle joint to a 2–4” post. Slide this post into a right-angle connector.

Author Manuscript Author Manuscript Author Manuscript Author Manuscript

7. Slide the IR light + post + connector onto the 12” post you screwed in before so that the light can be easily directed to the same point as the camera’s focal plane.
8. Connect the camera to the gigabit Ethernet card in the PC with the Cat6 Ethernet cable.
9. Connect the camera power supply.
10. Open Vimba Viewer or your camera’s video streaming software.
11. Stream video from your camera. Check that you can focus on the near headplate bar, which is approximately the depth where the mouse’s face will be. Check that the image is not too bright or too dark. Adjust the aperture/focus of your camera lens and the position of your camera until you find something that you like. Depending on the space available in your setup, you may find that you need a 10 mm or 5 mm extension lens to achieve the right focus and field of view. Experiment with the different extension tubes until you can to find a good video image.
12. Once the camera is set up in approximately the right location, test again with a mouse in the rig. Use the grayscale images shown in Fig. 2 as a guide.

2.4 Surgery

Materials

- Stereomicroscope with fiber-optic illumination (e.g., Zeiss Stemi 2000)
- Sterile physiological saline
- Sterile 1 mL syringes with needle
- Canned compressed air
- 7.5% povidone-iodine
- 70% ethanol
- C&B Metabond Quick Cement System (Parkell Inc. S396, S398, S371, S379, and S387)
- Dental acrylic (e.g., Lang Jet 1406, 1220)
- Depilatory cream
- Ophthalmic ointment or artificial tears
- Sterile nylon sutures (LOOK 18” Nylon Suture with C-17 needle, 5–0; ref. no. 917B)
- Antibiotic ointment
- Sterile gauze and cotton balls torn and rolled into 2–3 mm balls
- GELFOAM (Fisher Scientific NC04090659)
- Kwik-Sil (WPI Kwik-Sil)

Author Manuscript Author Manuscript Author Manuscript Author Manuscript

- Instruments
  - Precision jeweler screwdriver compatible with skull screws
  - Small scissors (e.g., Fine Science Tools (FST) 14094–11)
  - Small spatula (e.g., WPI 504022)
  - Curved forceps (e.g., Dumont #7 from FST 11271–30)
  - Curved serrated forceps (e.g., Dumont #7b from FST 11271–30) (file off one to two teeth to grip screws better)
  - Fine-tipped forceps with angle (e.g., Dumont #5/45 from FST 11251–35)
  - Dental drill (e.g., Osada EXL-M40)
  - 0.5 mm burr drill bits compatible with dental drill
- 1/mouse, headplates (1” × 5/16” × 1/32”) (custom machined from titanium or stainless steel; schematic available at http://github.com/blinklab)
- Custom headplate adapter (Fig. 3)
- 3D printed custom recording chamber (Fig. 5g; can be 3D printed by NeuroNexus Technologies or similar; schematic available at http://github.com/blinklab) or plastic ring that can serve as a recording chamber
- Skull Screws (e.g., Antrin Miniature Specialties, Inc. AMS120–1B, 000–120×1/16 SL BIND MS SS)
- Small animal stereotaxic surgical rig (Kopf 930)
- Universal stereotaxic adapter (e.g., Kopf Model 1772)
- Stereotaxic adapter for implanting cannulae (e.g., Kopf model 1766-AP)
- Silver wire (optional)

2.5 Eyeblink Conditioning

Materials

- Data acquisition and stimulus delivery system. For example:
  - TDT RZ5
  - TDT Medusa preamp with high impedance headstage such as RA16
  - TDT P05e PC interface card
  - TDT zBus ZB1PS Caddy
  - Multi-Field Magnetic Speakers (TDT MF1) (Fig. 1a)
  - Stereo power amp for speakers (TDT SA1)

Author Manuscript Author Manuscript Author Manuscript Author Manuscript

  - Windows PC with specs good enough to run the software and handle the video frames in near real time (e.g., 3.4 GHz Core i7 CPU and 16 GB RAM)
  - BNC to LED cable with ~330 Ohm resistor for LED (Fig. 1b)
  - One pressure injector (Applied Scientific Instrumentation MPPI-3)
  - One 23G blunt needle (Fig. 1e)
  - Tubing for air puff delivery (Clippard URH1–0402-CLT) (Fig. 1e)
  - One plastic 1/16” barbed to luer fitting to couple the blunt needle and air puff tubing (e.g., WPI 13160) (Fig. 1e)
  - Sound pressure meter (optional)
  - MATLAB (or other data processing software)
  - Neuroblinks software from http://github.com/blinklab (for use with MATLAB and TDT, may be substituted with other behavioral training software)
- Nitrogen gas with regulator
- 1/stimulus location, ½ diameter post (6–12” length, depending on your preferred setup)
- 1/stimulus, third hand (e.g., alligator clip and stem from SUNYEE Helping Hand MZ101B)
- 1/stimulus, right-angle mounts that can accommodate the third hands (OptoSigma CCHN-12.7–6 is compatible with SUNYEE Helping Hand)
- Air pressure measurement tool (e.g., PCE Instruments, PCE-P50; or construct your own based on a barbed pressure sensor like Honeywell SSCDANN150PG2A3)
- Tubing that will fit the pressure sensor barb and the luer adapter in the US delivery tubing (e.g., Clippard URH1–0804-CLT)

Construction

1. For each stimulus, screw a ½” diameter post somewhere around the front of the treadmill.
2. Attach the stimulus to the post using a right-angle mount, third hand, or other appropriate connector. Position the stimulus so that the mouse can reasonably be expected to perceive it.
3. Connect the various stimuli that you are using to the stimulus triggering/data acquisition hardware. Interface with the appropriate software. If you are using the TDT RZ5 system, you can use the Neuroblinks software from this laboratory listed above.

Author Manuscript Author Manuscript Author Manuscript Author Manuscript

2.6 Electrophysiology

Materials

Apparatus

- Stereotaxic micromanipulator (e.g., Narishige SMM-100 with custom shaft (EDMS16–054b) and modified MA-2 micromanipulator stand (SDMS16–033a)) (Fig. 1j)
- One-axis micromanipulator (e.g., Narishige MMO-220A one-axis oil hydraulic micromanipulator modified to remove the ball joint) (Fig. 1i)
- Handheld microscope camera (Dino-Lite AD-4013 MTL) (Fig. 1h)
- Adapter for microscope camera (Dino-Lite HD-P1)
- Three-axis manipulator for microscope camera (e.g. Narishige UMC3) (Fig. 1g)
- 10 mm OD post (if you use the UMC3)
- 7 mm OD post (for holding the camera adapter in the micromanipulator)
- Four ½” diameter 12” posts (Thorlabs)
- Two ½” diameter 6” posts (Thorlabs)
- Three right-angle mounts for ½” posts (Thorlabs RA90)
- 1/stimulus, third hand (e.g. alligator clip and stem from SUNYEE Helping Hand MZ101B)
- 1/stimulus, right-angle mounts that can accommodate the third hands (OptoSigma CCHN-12.7–6 is compatible with SUNYEE Helping Hand)
- Solid core copper ground wires and panel

Supplies

- Custom dura scraper (see Fig. 3e, f)
- Sterile saline
- Small cotton balls
- 7.5% povidone-iodine
- Electrodes (see Note 6)
- Optrodes (see below for construction instructions)
- Implantable optical fibers (e.g., Thorlabs or custom-made)

Construction of the Recording Apparatus

1. Attach your materials to the vibration isolation table in appropriate positions relative to the treadmill using the Thorlabs posts and RA90 right-angle

Note 6. Choosing an Electrode

Author Manuscript Author Manuscript Author Manuscript Author Manuscript

connectors. Make sure everything is very stable and screwed tightly down onto the breadboard. See Fig. 1 for example arrangement.

2. Install the software to run the Dino-Lite camera. Position the camera so that it can focus at the height of the mouse's craniotomy and so that it will not block your micromanipulator from moving freely around the craniotomy.

3. You will need to use a mouse with a headplate and craniotomy to make sure that the positions of all your devices are appropriate for your purposes.

Eliminating Electrical Noise

- Depending on the specific features of your setup, you may have more or less ambient electrical noise. To counteract noise coming from outside of your recording rig, it can be helpful to place a Faraday cage around the rig or to work in an electrically shielded room. However, most of the noise you encounter will probably originate from the equipment you are using for your experiment. Here are some tips for ways to deal with this kind of noise.
- Ground everything to a single point.
- Use a stainless steel or copper braided mesh to shield all of the power cables going to your rig (e.g., McMaster 5537K14). Ground these.
- Wrap other sources of noise in aluminum foil and ground these.
- Make sure that all of your ground points are sitting at the same voltage to eliminate potential ground loops.
- Electrostatic discharge from the mouse can be another noise source. Place the equipment out of the mouse's reach. If impossible (e.g., air puff needle, reward tubing, etc.), the object can be electrically connected to the mouse, or both the object and the mouse can be connected to the ground.
- Vibration is another potential noise source. The wires and clips between the headstage/preamp and the mouse and the ground wire should be stabilized.

2.7 Optogenetics

Materials

- Implantable Fiber Optic Cannulae (can be purchased from multiple vendors, including Thorlabs and Doric Lenses or constructed following the *Thorlabs Guide to Connectorization and Polishing of Optical Fibers*; *see* Notes 2 and 3)
- Laser or LED with driver for supplying fixed wavelength illumination (e.g., Blue Sky Research or Thorlabs)
- 100 or 200 μm optical fiber with silica cladding (if not purchasing preassembled, e.g., Thorlabs FG105LCA or FP200URT)

Note 2. Optical Fibers
Note 3. Constructing Optical Fibers

Author Manuscript Author Manuscript Author Manuscript Author Manuscript

- 1.25 mm Zirconia ferrules with ID matching optical fiber (if not purchasing preassembled, e.g., Kientec FAZI-LC-230)
- Patch fiber with same diameter as implantable fiber for transmitting light between laser and implanted fiber (e.g., Thorlabs FG200UCC; or can be made by hand)
- Butane torch
- Stainless steel hypodermic tubing (e.g., 23XX and 26RW gauge) to protect the optical fiber and provide rigidity (optional, if making long optical fibers for acute use (see below))
- Light meter (Thorlabs PM100D and S140C)

Pulling Optical Fibers for Use in Acute Preparations—Connectorized optical fibers that have a silica cladding can be heated and pulled to produce finer tip sizes that allow the fiber to more easily pass through the dura and provide more precise targeting of cell populations [7, 21] (Fig. 4). Once pulled, they can be glued to an electrode to make a custom "optrode." Fine control over the pull can be achieved using a pipette puller capable of melting quartz glass, such as a Sutter P-2000. However, with practice, optical fibers can be manually pulled by heating them over a small butane torch. To manually pull an optical fiber, start with a connectorized optical fiber that extends at least four inches from the unpolished end of the ferrule (Fig. 4a). Hold the center of the fiber vertically in front of the flame, gripping the ends with forceps or pliers in each hand, with the connectorized end on top (Fig. 4b). Gently pull the ends apart until the glass becomes fluid and starts to give (Fig. 4c). Then simultaneously remove the fiber from the flame while rapidly pulling the ends apart (Fig. 4d). If done properly, the fiber will taper to a submicron diameter, and then the two ends will break away from each other. At this point the tip is usually too small to be useful, so use a diamond or ruby scribe to cleave the connectorized fiber along its taper to the desired diameter. We typically use fibers with ~20 μm tip diameters (Fig. 4f). The cleaved end can be sharpened by holding it at an acute angle against the rotating surface of a pipette beveling device or hard drive platter covered with fine grit polishing paper. A conical tip shape can be produced by gently rotating the fiber about its long axis as it contacts the polishing paper, but bear in mind that this will remove the cladding at the tip of the fiber and allow light to leak out along the cone. Glue the optical fiber inside appropriately sized hypodermic tubing to protect it and make it more rigid, leaving at least 5 mm of the tip exposed (Fig. 4e).

Testing Optical Fiber Light Transmission

1. Connect light sensor (e.g., Thorlabs S140C) to the meter (e.g., Thorlabs PM100D), and power up the system.
2. Connect a patch fiber to the laser and point at the light sensor. urn on the laser.
3. Move the light-emitting end of the patch fiber so that the light sensor reaches its maximum reading. Record this value. Turn off the laser.

Author Manuscript Author Manuscript Author Manuscript Author Manuscript

4. Connect your optical fiber to the patch fiber. Repeat step 3, this time with the optical fiber instead of the patch fiber.

3 Methods

3.1 Surgical Procedures

Two separate surgical procedures are required to prepare mice for head-fixed single-unit extracellular recording: (1) implantation of a headplate for head fixation and (2) drilling of a craniotomy and implantation of a recording chamber. These procedures can be performed during the same surgery or separated by several weeks, depending on your experimental needs and institutional protocol.

3.1.1 Anesthesia and Preoperative Care—Inhalation anesthesia is induced by 5% isoflurane (% by volume in O2; SurgiVet) and maintained with 1.0–2.0% isoflurane throughout the surgery. Mice are placed in a stereotaxic apparatus (*see* Note 4.1), and a nonsteroidal anti-inflammatory drug (e.g., meloxicam) is given subcutaneously to reduce swelling and provide analgesia. During surgery, core body temperature is maintained by placing the mouse on a heating pad (DC temperature controller, FHC) to prevent hypothermia. Both eyes are covered with “artificial tears” ointment to keep them moist. Fur over the surgical site is removed by electric clippers and depilatory cream. The skin is then cleaned by three alternating scrubs of povidone-iodine surgical scrub followed by 70% alcohol.

3.1.2 Stereotaxic Implant of Headplate and Ground Screw—Surgery is performed under a stereomicroscope with fiber-optic illumination. A midline incision is made to expose the skull, and the underlying periosteum is cleared with cotton swabs so that bregma and lambda can be clearly seen. Two layered muscles attached to occipital bone (the splenius capitis and trapezius, Fig. 5e, f) are detached at their insertion point, reflected back, and covered by sterile Kimwipes or cotton balls to obtain a clear surgical field. To position the mouse in the stereotaxic plane (as defined by Paxinos and Franklin [22]), the midline suture should be aligned parallel to the anterior/posterior axis of the stereotaxic manipulator arm. The head of the mouse should be rotated around the ear bar axis (pitch) so that the dorsal/ventral difference between bregma and lambda is less than 50 μm. A shallow outline is then drilled to mark the craniotomy location that targets EBC-related areas (2–3 mm diameter craniotomy centered 6.5 mm posterior and 2.0 mm lateral from bregma, Fig. 5a). This area includes several lobules of the cerebellar cortex, including paravermal IV/V and

Note 4.1. Securing the mouse in ear bars stabilizes the skull, and skull stability is important when stereotactically implanting in multiple locations on the skull. Using non-rupture ear bars for mice (e.g., Kopf 822) will facilitate pitch adjustments for achieving a stereotactic plane.
Leveling the skull will be the easiest/fastest if the mouse is secured in ear bars such that:

- The mouse’s head pitch can be easily and smoothly adjusted.
- The mouse’s head yaw cannot be adjusted with gentle pressure.
- The mouse’s nose is straight.
- The interaural distance is ~8 mm. If you are obtaining interaural distance measurements much smaller than this, you run the risk of damaging the ear canals (which could affect conditioning using tone stimuli) or compressing the airway.

Author Manuscript Author Manuscript Author Manuscript Author Manuscript

VI, and hemispheric simplex and crus I, as well as the inferior colliculus (Fig. 5h). If an optical fiber or guide cannula is to be implanted, also mark their target locations using the drill. Next, two screw holes are drilled on either side of the midline just posterior of bregma (being careful to not puncture the dura, Fig. 5a), and two #000–120 self-tapping stainless steel screws are screwed into the holes (Fig. 5b), using the curved forceps with filed teeth to hold the screw. A third hole is drilled into the interparietal bone contralateral to the craniotomy site, and a #000–120 stainless steel screw is screwed into this hole (Fig. 5a, b). The third screw serves as both an anchor for the cement to provide more stability for the implant and as a reference for the extracellular recording. A short length of bare silver wire can be connected on/around the third screw and covered with conductive epoxy to enable easy access to the reference screw (Fig. 5d). Next, the screws and most of the dorsal surface of the skull are covered in cement, leaving only the future location of the craniotomy clear (C&B Metabond, Fig. 5b). A custom-made stereotaxic adapter (Fig. 3a–d) is used to hold the headplate (Fig. 3c) in the stereotaxic plane such that the headplate can be held securely in place over bregma, while dental cement is applied (transparent dental acrylic or Metabond, Fig. 5c) to a very dry bone surface (*see* Notes 4.2 and 4.3) using a small spatula (e.g., WPI 504022). When the dental cement is almost completely cured, a small indentation is placed over bregma using the stereotaxic adapter's retractable stylus. The indentation will be used as a reference mark for guiding recording tracks based on stereotaxic position. Once the cement has fully cured and is hard to the touch, the headplate adapter can be removed.

3.1.3 Craniotomy and Recording Chamber—The craniotomy is drilled along the previously marked outline. To avoid puncturing the dura, it is crucial to make the craniotomy very slowly, gradually removing thin layers of bone and stopping periodically to irrigate the tissue with sterile saline. The saline should be blotted away with small cotton balls and any bone dust blown away with compressed air. Once the bone has been cut through along the entire perimeter of the craniotomy, the remaining bone flap should feel loose when gently pushed with forceps. At this point, the bone flap can be gently pulled away from the dura with fine-tipped, angled forceps, taking care to avoid rupturing blood vessels near the surface of the dura. Wetting the bone and dura with saline for a few minutes before attempting to lift off the flap can make it easier to remove and reduce trauma. The exposed dura is covered with a thin layer of silicone elastomer (Kwik-Sil, WPI) to protect it between recording sessions (see Sect. 3.1.6). Next, a plastic recording chamber (Fig. 5d, g) is placed on the craniotomy site and secured by dental acrylic. This chamber serves two purposes: (1) it protects the dura between recording sessions by preventing debris from entering the craniotomy and holding the silicone elastomer in place, and (2) it serves as a bath to maintain saline on top of the dura during recording sessions.

Note 4.2. In order to increase the available surface area for dental cement to bind to, the surgeon can use Dumont #7 forceps or any other suitable surgical instrument to score the skull. This should be done carefully, however, as the mouse skull can be easily punctured, especially in the more anterior regions.

Note 4.3. The skull should be very clean and thoroughly dry when dental cement is applied. Moisture trapped between the dental cement and skull will (1) prevent the dental cement from bonding to the bone and (2) facilitate infection and bone decay by making pockets for bacteria to colonize. This second point is particularly relevant around the margins of the dental cement. To aid in drying the skull, the surgeon can use canned air. It can also be helpful to wipe the skull with a cotton swab moistened by hydrogen peroxide or 70% EtOH, although this should only be done as long as the skull is intact (i.e., you have not made any holes in the skull) in order to avoid damaging the brain. The surgeon should monitor the margins of the dental cement while it cures, drying any interstitial fluid or other seepages from the incision before it can contact the curing dental cement.

Author Manuscript Author Manuscript Author Manuscript Author Manuscript

3.1.4 Implantation of Chronic Optical Fibers and Guide Cannulae—The principles underlying the implantation of chronic optical fibers or guide cannulae for drug delivery are essentially the same. After preparing and leveling the skull as described in Sect. 3.1.2, a small craniotomy is drilled over the stereotactic coordinates of the target. The implant is secured in the appropriate stereotaxic attachment (e.g., Kopf 1766-AP for guide cannulae or Kopf 1772 holding a pin vise for optical fibers). Then, a small incision is made in the dura using a sharp tool or sterile needle so that the implant can easily enter the brain instead of deforming the tissue. The implant is lowered to the desired depth. After verifying that the skull is very dry (*see* Note 4.3), a small spatula is used to apply Metabond around the implant, leaving enough of the implant free of Metabond to attach dummy cannulae or fiber-optic patch cables.

3.1.5 Completion of Surgery and Postoperative Care—Any remaining wound from the midline incision should be sutured and a topical antibiotic applied to the wound margins. In the first week following surgery, mice should be monitored twice daily. Topical antibiotics should be applied to the wound to prevent infection, and analgesics should be delivered according to your laboratory's approved animal protocol. Careful attention should be paid to the general level of activity of the mouse, including grooming behavior, vocalization, respiration, urination, defecation, eating, and drinking. In addition, the mice should be monitored for any signs of ataxia (one of the cardinal symptoms of damage to the cerebellum). Mice that develop ataxia should be euthanized.

3.1.6 Maintaining the Craniotomy and Health of the Dura—Covering the craniotomy with a silicone elastomer dramatically improves the health of the dura and prevents scar tissue buildup and reossification. Despite this, it is occasionally necessary to remove excess scar tissue or bone from the dura before performing a recording experiment. Once the original silicone plug has been removed and experiments have begun, we use an antiseptic (povidone-iodine) to clean the craniotomy daily before and after each recording session to keep it in good condition.

To access the craniotomy for cleaning, the chamber lid is opened, and povidone-iodine is applied into the chamber on the surface of silicone elastomer. The povidone-iodine is left in place for at least 1 min and is then removed with small sterile cotton balls (2–3 mm, torn from larger cotton balls) before opening the silicone. The silicone is removed by gripping it along its edge with curved forceps and gently lifting it away. After removing the silicone, povidone-iodine is applied to the dura and left to sit for a few minutes. Excess povidone-iodine solution is then removed with small sterile cotton balls, and the chamber is rinsed with sterile saline. At this point the dura can be examined to determine if the brain is acceptably visible or if there is excess bone or scar tissue buildup that needs to be removed before recording. If the dura is transparent and all blood vessels and cerebellar lobules are visible, the dura is usually thin enough to skip the dura cleaning step. If the dura is thicker, the excess granulation tissue can bend or otherwise damage the tip of the electrode. The granulation tissue is carefully removed by scraping off thin layers with a handmade tool (made from FST forceps, Fig. 3e, f) being careful not to rupture the dura. Stop when the dura and vasculature are visible. Saline is then applied into the chamber to keep the dura

Author Manuscript Author Manuscript Author Manuscript Author Manuscript

moist. A local anesthetic can be added to the saline solution (1% lidocaine) to reduce pain when the mouse wakes up.

After the experiment, the dura should be cleaned with povidone-iodine again, followed by a sterile saline rinse. Last, a thin layer of silicone elastomer (Kwik-Sil, WPI) is applied and the chamber closed with a disinfected lid. Using these procedures, a healthy dura can be maintained for more than 1 month (Fig. 5h).

It is also beneficial to trim the fur on the dorsal surface of the neck on a weekly basis to prevent fur from entering the chamber when the mouse hunches its shoulders on the treadmill. Fur entering the chamber can provide a route for infection and can be a source of electrical artifacts during recording.

3.2 Eyeblink Conditioning

Eyeblink conditioning can be carried out using stimulus delivery and data collection hardware and software like those described in *Materials*. It is essential that stimulus delivery be performed with at least 1 ms precision and that stimulus delivery, behavioral data, and electrophysiological data be timestamped according to the same clock.

To reduce stress during training sessions, the mouse is habituated to the conditioning apparatus. During this phase of the experiment, the animal is head-fixed (*see* Note 5.1) atop the treadmill via the headplate and bar system for 1 h/day until the mouse can walk comfortably on the wheel and maintains a normal posture (*see* Note 5.2). This process normally takes 2–3 days. All features of the apparatus and environment should be identical between the habituation sessions and normal training sessions, with the exclusion of CS and US presentation (*see* Note 5.3).

Following habituation, EBC sessions can begin. The mouse is once again head-fixed atop the treadmill in the conditioning apparatus. The CS may be any neutral stimulus that your system can deliver (e.g., LED illumination, a pure tone, etc.). The relative timing of the CS and US presentations (interstimulus interval, ISI) can be altered to engage different brain structures in the task. To train mice using a delay EBC paradigm that recruits the cerebellum [12, 16, 17], the US is presented while the CS is still on. Using a light CS, mice can effectively learn to make CRs in delay EBC with ISIs between approximately 200 and 500 ms [11]. To train mice using a trace EBC paradigm that recruits the cerebellum and other brain areas, including dorsal medial prefrontal cortex, hippocampus, and amygdala [23], the US is presented 200–500 ms after the CS terminates. During both delay and trace conditioning, trials are typically delivered at 10–25 s intertrial intervals (*see* Note 5.4). Mice are typically trained for at least 100 trials/day (*see* Note 5.5). EBC can be carried out using

Note 5.1. If you observe the mouse's eye moving up/down/ side to side substantially while he is head-fixed, the headplate may be loose. Remove the animal from the rig, and ascertain in a surgical setting whether the headplate can be secured to the skull better or whether the animal must be euthanized.

Note 5.2. Make sure that the mouse fits comfortably on the treadmill (i.e., the mouse reaches the surface of the wheel without trouble, the mouse is not squished against the wheel, the wheel spins freely).

Note 5.3. Making changes from the habituation conditions can dishabituate and frighten the animals. This includes playing masking white noise (or not) at the same volume level from day to day, positions of the different CS and US delivery mechanisms, etc. In addition, keep the positions of all parts of the conditioning apparatus as consistent as possible throughout your experiment to make sure that features of the stimuli do not differ between trials or sessions with the same mouse.

Author Manuscript Author Manuscript Author Manuscript Author Manuscript

100% CS + US trials. However, it can be informative to include some (e.g., 20%) CS-only trials (*see* Note 5.6). These trials allow the experimenter to examine the CR without interference from the UR. This is important, as the peak of the CR occurs after the US is delivered [11], and CR peak time is an important factor for assessing cerebellum dependency (see Sect. 3.8.2 for more details). When designing the EBC paradigm, the experimenter should consider whether it is important to use CS-only trials and whether delivering CS-only trials will confound the research question.

Depending on task parameters such as ITI, puff strength, and ISI, mice should start showing CRs within 2–3 days of training [12]. If a mouse does not start showing CRs within this period, verify that there are no problems with the conditioning apparatus or stimulus delivery parameters. If there are no clear problems and the animal has not acquired any conditioned responses within 5 days of training, it is best to start working with another mouse (*see* Note 5.7).

US intensity affects the rate of learning and the degree to which the learning depends on the cerebellum. Using a stronger US during task learning may recruit the amygdala [10, 24], and using a weaker US delays or fails to support learning of the eyeblink CR. If the US intensity decreases after CR acquisition, the CR may be partially or completely extinguished [25]. For consistent US intensities during training, the US delivery needle must be the same distance from the cornea each day, as the puff pressure at the cornea decreases with the square of the distance. The experimenter should also measure air puff strength (e.g., PCE-P50) to be sure that US intensity is appropriate (*see* Note 5.8). This laboratory has successfully used an air puff US with peak pressures from 6.5 to 8.5 PSI and positioned the US delivery needle ~3 mm from the cornea for cerebellum-dependent eyeblink conditioning (*see* Notes 5.9 and 5.10).

3.3 Acute Single-Unit Recording and Stimulation during Behavior

Acute single-unit recording or stimulation experiments can be performed daily during eyeblink conditioning sessions. Once the mouse is prepared for single-unit recording as described above, it is placed on the treadmill, and its head is fixed in place by the headplate. The session can begin after allowing approximately 10 min for the mouse to recover from

Note 5.4. Trials should not be delivered if the animal is too squinty (e.g., above 20% baseline eyelid closure), as this will make it difficult to detect CRs and can decrease the perceived strength of the US.

Note 5.5. The Neuroblinks EBC conditioning software used in this laboratory requires the experimenter to deliver one US-only trial at the beginning of each session. This calibration trial is used to extract the fraction eyelid closure in real time during the session (see Fig. 2). If delivering this calibration trial would confound the experimental question being addressed, the open source Neuroblinks software should be modified accordingly to suit the needs of the experiment.

Note 5.6. Including too many CS-alone trials during acquisition will delay/prevent learning. We would not recommend delivering more than 25% CS-alone trials. However, there is some evidence that rabbits can learn to make CRs during EBC with 75% CS-alone trials [53].

Note 5.7. Damage to the cerebellum during surgery or due to insult on the craniotomy can render animals incapable of learning the task, so be impeccable with your operative and post-op care.

Note 5.8. The time course of the air puff delivered will differ from the time course of the trigger sent to the pressure injector. The onset of the air puff will be delayed, with the duration of this delay depending on the length of tubing between the pressure injector and the puff needle. In addition, air puff pressure will peak after the time that the trigger ends. For example, in our system air pressure begins to rise 12 ms after trigger onset, and peak pressure for a 30 ms trigger is ~50 ms after trigger onset. You should test your system to ascertain the delay to puff peak and onset in order to better inform your experimental design.

Note 5.9. The US must be strong enough to elicit full eyelid closure during reflex blinks, but not so strong that it damages the cornea. As a rule of thumb, the puff should produce a reflex blink with about 100 ms of complete eyelid closure.

Note 5.10. Test the pressure injection system for the US regularly.

Author Manuscript Author Manuscript Author Manuscript Author Manuscript

anesthesia. The electrode (*see* Note 6) is lowered into the recording chamber under visual inspection with a stereomicroscope or Dino-Lite digital microscope. The anteroposterior and mediolateral locations of recording tracks are determined relative to the mark placed above bregma during the headplate surgery. The surface of the dura serves as the dorsal-ventral reference position.

The general strategy we use is to make recording tracks at evenly spaced intervals (100–200 μm) along the anteroposterior and mediolateral axes in a grid pattern. This ensures good coverage of the target region and is especially valuable during initial mapping experiments (see below). By taking care to place the mouse in the headplate holder consistently from day to day, the same region can be reliably targeted daily based on stereotaxic coordinates or visible surface landmarks. Figure 8 shows recording data during EBC for an example Purkinje cell and an example DCN cell.

3.4 Identifying Cerebellar Layers and Cell Types

The cerebellar cortex consists of three distinct layers that can be identified based on their characteristic activity profiles [26, 27] (Fig. 6): (1) molecular layer, (2) Purkinje cell layer, and (3) granular layer. These layers are comprised of different cell types and processes, giving each a distinct electrophysiological signature. When recording in the cerebellar cortex, it can be useful to listen to the auditory features of the recorded data. Listening to the activity can be perplexing at first, but over time the experimenter develops an ear for the different characteristic sounds of the cerebellar cortical layers.

The molecular layer contains the Purkinje cell dendrites, granule cell axons (parallel fibers), and molecular layer interneurons. When the electrode tip is in the molecular layer, recordings contain almost exclusively prominent complex spikes from the Purkinje cell dendrites and otherwise quiet background activity [27, 28] (Fig. 6a). Complex spikes are the postsynaptic response of Purkinje cells to inputs from the inferior olive and have a distinct discharge rate of approximately 1 Hz [29]. Complex spikes make a characteristic popping sound (like popcorn kernels popping). Other action potentials arising from molecular layer interneurons can occasionally be found, but the signals are typically smaller than complex spikes and more difficult to isolate.

The Purkinje cell layer contains densely packed Purkinje cell bodies that each emit high-frequency simple spikes and low-frequency complex spikes, giving recordings in this layer a high back-ground activity (Fig. 6b). Complex spikes are recognizable by their characteristic low-frequency (~1 Hz) discharge and the presence of calcium spikelets [29, 30] (Fig. 6b, *right*), which contribute to the “popping” sound. Simple spikes are characterized from other action potentials by at least three criteria: (1) the mean spontaneous firing rate of simple spikes should range from 50 to 100 Hz [29], (2) simple spikes should pause briefly after complex spikes (10–30 ms) [29, 31] (Fig. 6b, *inset*), and (3) simple spike amplitude should be roughly comparable with complex spike amplitude (though the most prominent direction —positive or negative—of the simple and complex spikes can sometimes vary considerably). If these simple spike criteria are not met, then the recording may be missing Purkinje cell action potentials, or the recording may contain multiple units.

Author Manuscript Author Manuscript Author Manuscript Author Manuscript

The granular layer contains the tiny, densely packed granule cells, mossy fiber terminals, and cell bodies of Golgi cells and other granular layer interneurons [26]. The granular layer cells receive much of their synaptic input in glomeruli that are innervated by mossy fiber terminals (called rosettes). The mossy fiber rosettes are often larger than granule cell bodies and may contribute to a characteristic “hashy” sounding background activity in the granular layer. Interneurons, such as Golgi cells, can often be isolated in the granular layer or heard in the background (Fig. 6c). Criteria have been developed in anesthetized animals to identify some of the cerebellar cortical interneurons based on their spike patterns, but it remains to be seen whether these criteria translate to the awake mouse [32, 33].

The cerebellar cortex surrounds the deep cerebellar nuclei, which are mostly identified based on depth and absence of the characteristic signatures of the cortex (Fig. 6d).

3.5 Using Sensory Stimulation to Map Climbing Fiber Receptive Fields

The cerebellar cortex is organized into microzones, which are longitudinal bands in which Purkinje cells are innervated by climbing fibers with similar sensory receptive fields [34]. The microzones can be mapped by recording climbing fiber responses to stimulation of different points on the body surface to determine the receptive field [35, 36, 37]. Climbing fiber responses can be recorded as either single-unit complex spikes or as evoked potentials within a local field potential (low-pass filtered, 300 Hz cutoff; Fig. 6a, b and 7a), and in our experience, there is a strong correlation between the climbing fiber receptive fields identified by these two methods. It is best to begin mapping using stereotactic coordinates, but you should ultimately rely on recorded responses to sensory stimulation to determine whether the electrode tip is in a microzone of interest (e.g., Fig. 7a). In practice, local field potential recording is more useful for coarse mapping, and single-unit recording is more useful for finer-scale mapping. However, the source of the local field potential is still unclear, and the signal can be contaminated by non-climbing fiber sources, such as those arising from the mossy fiber pathway [36], so more care must be taken in interpreting the local field potential recordings.

As an additional precaution, stimulation trials should only be started when the animal is not moving (without locomotion, face grooming, licking, etc.) because the local field potential is easily contaminated by movement artifacts.

3.6 Using Microstimulation to Map DCN Motor Outputs

Unlike in the cerebellar cortex, there are no accepted criteria for identifying the different neuron classes of the cerebellar nuclei based on extracellular recordings. These neuronal classes include large excitatory projection neurons and smaller inhibitory neurons that make local synaptic contacts and/or project to the inferior olive or cerebellar cortex [38]. However, due to their substantially larger size, the excitatory projection neurons are more likely to be isolated in an extracellular recording, and we often assume these are the majority of the neurons that we record.

Because the excitatory projection neurons of the DCN project to premotor structures, including various brainstem and midbrain nuclei, the DCN can be functionally mapped by using microstimulation to elicit movements [39]. This is particularly true for the anterior

Author Manuscript Author Manuscript Author Manuscript Author Manuscript

interposed nuclei (AIP), which is where the essential region for eyeblink conditioning is located [12, 17]. The movements evoked by microstimulation in a particular location within the AIP give a reasonable estimate of the underlying somatotopic representation and a clue about the climbing fiber receptive fields of the Purkinje cells that project there [40].

Microstimulation is performed through platinum/iridium or tungsten microelectrodes that typically have lower impedances than what would be used for recording (in the range of 50–100 KOhms), but higher impedance recording electrodes can also be used if desired. We typically use a monopolar stimulation configuration in which the reference lead is attached to the same implanted reference screw used for recording, but bipolar stimulating electrodes can be used as well and may help contain the current spread, particularly at higher stimulation intensities. The stimulating electrode should be attached to the positive lead of a stimulus isolation unit capable of delivering currents in the range of 1–50 μA through the electrode. The stimulator should be configured to deliver biphasic pulses (pulse width 200 μs for each phase) at 200–500 Hz for train durations up to 500 ms. We have found that 200 ms pulse trains at 500 Hz reliably and reproducibly evoke movements that are easy to detect with high-speed videography (e.g., Fig. 7b) but that longer train durations can make the movements more clear to the naked eye. Microstimulation mapping begins when the electrode is positioned approximately 500 μm above the expected depth of the DCN, typically in the overlying cerebellar cortex or white matter. Stimulation at this depth with currents around 15–20 μA can evoke a variety of movements, but these movements are often non-specific and probably result from antidromic activation of motor-related mossy fibers projecting to the cerebellar cortex [41]. As the electrode is advanced toward the DCN, the ability to evoke movements with microstimulation intensities below 20 μA will briefly diminish and then will increase as the electrode enters the DCN. Within the DCN, microstimulation intensities as low as 1–2 μA are often sufficient to evoke motor twitches, but discrete movements usually require currents between 5 and 10 μA. Once the threshold current is found for evoking movement at a particular depth within the DCN, the electrode should be advanced 50–100 μm and the threshold movement tested again (Fig. 7b). This is continued through the entire depth of the DCN at multiple rostral-caudal and mediolateral locations such that a somatotopic map of evoked movements can be compiled. The essential location for eyeblink conditioning within AIP is identified based on the ability to evoke discrete eyelid closure with low currents (5–10 μA) [12]. Once this “hot spot” is identified, it can be targeted for single-unit recording.

3.7 Acute Optogenetics and Electrophysiological Recording During Behavior

Photostimulation during extracellular recording is a powerful technique for identifying genetically defined cell classes [42], relating optogenetically induced changes in neural activity with coincident changes in behavior [7, 43–45], or simply confirming that an optogenetic manipulation has the desired effect on neurons within the circuit [46]. We perform combined photostimulation and recording in awake mice using custom-made “optrodes” that consist of a length of optical fiber that is connectorized to a ferrule at one end and pulled to a fine tip at the other (Fig. 4). The fiber is then reinforced by placing it inside hypodermic tubing and attached to a tungsten electrode using cyanoacrylate glue. Once assembled an optrode can typically be used for multiple penetrations across multiple

Author Manuscript Author Manuscript Author Manuscript Author Manuscript

days until the electrode impedance drops too much to maintain single-unit isolation. When this happens, the electrode can be removed by gently heating the assembly with a heat gun and separating it from the optical fiber. The optical fiber can then be attached to a new electrode, and this can be repeated until the optical fiber becomes too damaged to transmit light. See Materials for a description of how to measure light transmission through the optical fiber.

During an experiment, the optrode is lowered into the brain using a micromanipulator, as with the normal single-unit extracellular recording procedure described above. The only additional requirement is that the optical fiber must be coupled to a fixed wavelength light source, such as a laser or LED. Be aware that photostimulation can sometimes induce artifacts in the recording due to the photoelectric effect [47]. This can be partially mitigated by ensuring that bright light coming from the fiber optic does not directly illuminate the electrode surface.

3.8 Data Analysis

A full description of data analysis is outside the scope of this chapter. However, in this section, we provide some guidelines for basic analysis of neural and behavioral data that are relevant for the cerebellum and EBC.

3.8.1 Spike Sorting—The best way to ensure that you are only picking up the activity of a single neuron is to take your time positioning the electrode during the experiment so that the spikes of a single neuron appear several times larger in amplitude than spikes from the surrounding neurons. If you have achieved “single-unit isolation,” the spikes can be detected and stored during the experiment using a time-amplitude window discriminator (either hardware or software based, depending on the data acquisition system). However, it is sometimes possible to use post hoc (“offline”) spike sorting algorithms based on principal component analy+sis (PCA) or direct measurements of spike features to separate the signals from multiple units that were picked up on the same electrode [48, 49]. Offline spike sorting can also be used to separate simple and complex spikes in a single-unit Purkinje cell recording [30].

There are several steps involved in sorting spikes, some of which depend on the particular properties of the cell type. Here we focus on sorting simple and complex spikes of a Purkinje cell. In an extracellular recording, simple spikes typically appear as brief negative and/or positive deflections in the extracellular field potential that last for only 200–300 μs (Fig. 6b). On the other hand, complex spikes begin with a similar brief deflection in the field potential that is then followed by a train of “spikelets” or low-frequency oscillations in the field potential that can last for up to several ms (Fig. 6b, *right*). Based on these differences in features, it is often possible to separate simple and complex spikes (Figs. 6b and 8a). First, the simple and complex spikes are extracted from the background activity generated by nearby neurons by setting an amplitude threshold. Next, exemplar simple and complex spikes are examined to determine promising criteria for distinguishing them. Often, a distinguishing feature is the deflection in field potential that occurs in complex spikes just following the rapid deflection that is shared by both simple and complex spikes. Using

Author Manuscript Author Manuscript Author Manuscript Author Manuscript

template matching, PCA, or other automatic methods for this period is often enough to obtain good spike sorting. Unfortunately, some complex spike profiles are difficult to sort using automatic methods, particularly when the initial phases completely overlap with those of simple spikes and the only distinguishing characteristic is the presence of spikelets. This is because the timing of spikelets is not the same from spike to spike, and automatic spike sorting algorithms are not good at dealing with time-jittered components. But for the trained eye, spikelets are obvious and easy to pick out, so complex spikes with these characteristics can be manually sorted.

Regardless of the method used, detected complex spikes should always be checked by eye, using the presence of spikelets or low-frequency oscillations to positively identify complex spikes. Once simple and complex spikes are sorted, it is essential to verify that they were emitted from the same neuron by generating a complex spike-triggered histogram of simple spike times. Presence of a 10–30 ms pause in simple spikes following each complex spike is the gold standard for showing that the simple and complex spikes were generated by the same Purkinje cell and is confirmation that the Purkinje cell was well isolated (Fig. 6b, *inset*).

3.8.2 Analyzing Behavioral Data—Eyelid movements are monitored using a high-speed camera (200 frames/s) and near real-time processing of the video stream to extract the eyelid movement trace over time. You can write your own software for this, or if you are incorporating MATLAB into your experimental setup, you can use our software (Neuroblinks, see *Materials*). If you choose to write your own software, you can use the following algorithm to measure eyelid movements (Fig. 2).

1. Select a region of interest (ROI) in your video, and discard information outside of the ROI in each frame. Select as small a region of interest as possible while including the whole eye.
2. Convert the image to binary, setting the threshold for black/ whiteness so that the pupil and iris are black but the surrounding fur is white. You may need to adjust the lighting in the chamber to eliminate any shadows that prevent you from collecting clear images.
3. Sum the numerical values of the binary image (the number of white pixels, indicating fur). Normalize the values such that the summed pixels range between zero (eyelid fully open) and one (eyelid fully closed). This transforms the pixel values into units of “fraction eyelid closure” (FEC).

We typically extract the eyelid trace in near real time during the experiment to control the task, but the time resolution of these data is not usually good enough for further analysis. Instead, after the session, we re-extract and renormalize the eyelid traces from the saved video frames. After the eyelid trace is normalized (i.e., between 0 and 1 FEC) based on a trial in which the mouse produces a full blink (for instance, a US alone trial), data analysis can begin. Learning can be measured in terms of the percentage of trials on which a CR occurred (%CR), amplitude of eyelid closure during a CR, CR timing, CR velocity, etc. There are multiple ways to operationally define a CR. Our laboratory uses a criterion of a 10% eyelid closure. It is possible to analyze eyelid movements in terms of absolute eyelid

Author Manuscript Author Manuscript Author Manuscript Author Manuscript

closure. However, mice sometimes squint during EBC, which can be confused for a small CR if eyelid position is not measured relative to baseline.

When quantifying CRs, it is critical to consider the timing of the eyelid movement, as this parameter reflects the degree of the movement's dependence on the cerebellum (recall from Sect. 3.2 that US intensity during training affects the brain structures recruited during EBC). If an eyelid response reaches its peak amplitude before the end of the CS-US interval, the response is poorly timed and may not be cerebellum dependent [10–12, 50, 51]. Additionally, tone CSs elicit unlearned, cerebellum-independent startles that are reflected in eyelid movements peaking 15–30 ms after CS onset [10].

It can also be informative to examine movement velocity [11, 52]. To calculate CR velocity, take the derivative of the eyelid position trace across all time bins in a given trial.

References

1. Humphrey DR, Schmidt EM (1990) Extracellular single-unit recording methods. In: Boulton AA, Baker GB, Vanderwolf CH (eds) Neurophysiol. Tech. Appl. to Neural Syst Humana Press, Totowa, NJ, pp 1–64
2. Bryant JL, Roy S, Heck DH (2009) A technique for stereotaxic recordings of neuronal activity in awake, head-restrained mice. J Neurosci Methods 178:75–79. 10.1016/j.jneumeth.2008.11.014 [PubMed: 19073214]
3. Schonewille M, Khosrovani S, Winkelman BHJ et al. (2006) Purkinje cells in awake behaving animals operate at the upstate membrane potential. Nat Neurosci 9:459–61; author reply 461 10.1038/nn0406-459 [PubMed: 16568098]
4. Goossens HHLM, Hoebeek FE, Van Alphen AM et al. (2004) Simple spike and complex spike activity of floccular Purkinje cells during the optokinetic reflex in mice lacking cerebellar long-term depression. EurJ Neurosci 19:687–697. 10.1111/j.1460-9568.2003.03173.x [PubMed: 14984419]
5. Cheron G, Gall D, Servais L et al. (2004) Inactivation of calcium-binding protein genes induces 160 Hz oscillations in the cerebellar cortex of alert mice. J Neurosci 24:434–441. 10.1523/JNEUROSCI.3197-03.2004 [PubMed: 14724241]
6. White JJ, Lin T, Brown AM et al. (2016) An optimized surgical approach for obtaining stable extracellular single-unit recordings from the cerebellum of head-fixed behaving mice. J Neurosci Methods 262:21–31. 10.1016/j.jneumeth.2016.01.010 [PubMed: 26777474]
7. Heiney SA, Kim J, Augustine GJ, Medina JF (2014) Precise control of movement kinematics by optogenetic inhibition of Purkinje cell activity. J Neurosci 34:2321–2330. 10.1523/JNEUROSCI.4547-13.2014 [PubMed: 24501371]
8. Paré WP, Glavin GB (1986) Restraint stress in biomedical research: a review. Neurosci Biobehav Rev 10:339–370 [PubMed: 3095718]
9. Li S, Fan Y-X, Wang W, Tang Y-Y (2012) Effects of acute restraint stress on different components of memory as assessed by object-recognition and object-location tasks in mice. Behav Brain Res 227:199–207. 10.1016/j.bbr.2011.10.007 [PubMed: 22008382]
10. Boele H-J, Koekkoek SKE, De Zeeuw CI (2010) Cerebellar and extracerebellar involvement in mouse eyeblink conditioning: the ACDC model. Front Cell Neurosci 3:19 10.3389/neuro.03.019.2009 [PubMed: 20126519]
11. Chettih SN, McDougle SD, Ruffolo LI, Medina JF (2011) Adaptive timing of motor output in the mouse: the role of movement oscillations in eyelid conditioning. Front Integr Neurosci 5:72 10.3389/fnint.2011.00072 [PubMed: 22144951]
12. Heiney SA, Wohl MP, Chettih SN et al. (2014) Cerebellar-dependent expression of motor learning during Eyeblink conditioning in head-fixed mice. J Neurosci 34:14845–14853. 10.1523/JNEUROSCI.2820-14.2014 [PubMed: 25378152]

Author Manuscript Author Manuscript Author Manuscript Author Manuscript

13. Hilgard ER, Marquis DG (1935) Acquisition, extinction, and retention of conditioned lid responses to light in dogs. J Comp Psychol 19:29–58. 10.1037/h0057836
14. Schneiderman N, Fuentes I, Gormezano I (1962) Acquisition and extinction of the classically conditioned eyelid response in the albino rabbit. Science 136:650–652 [PubMed: 13908977]
15. Chen L, Bao S, Lockard JM et al. (1996) Impaired classical eyeblink conditioning in cerebellar-lesioned and Purkinje cell degeneration (pcd) mutant mice. J Neurosci 16: 2829–2838 [PubMed: 8786457]
16. Kim JJ, Thompson RF (1997) Cerebellar circuits and synaptic mechanisms involved in classical eyeblink conditioning. Trends Neurosci 20:177–181 [PubMed: 9106359]
17. McCormick DA, Thompson RF (1984) Cerebellum: essential involvement in the classically conditioned eyelid response. Science 223:296–299 [PubMed: 6701513]
18. Schonewille M, Gao Z, Boele H-J et al. (2011) Reevaluating the role of LTD in cerebellar motor learning. Neuron 70:43–50. 10.1016/j.neuron.2011.02.044 [PubMed: 21482355]
19. Aiba A, Kano M, Chen C et al. (1994) Deficient cerebellar long-term depression and impaired motor learning in mGluR1 mutant mice. Cell 79:377–388 [PubMed: 7954803]
20. Shibuki K, Gomi H, Chen L et al. (1996) Deficient cerebellar long-term depression, impaired eyeblink conditioning, and normal motor coordination in GFAP mutant mice. Neuron 16:587–599. 10.1016/S0896-6273(00)80078-1 [PubMed: 8785056]
21. LeChasseur Y, Dufour S, Lavertu G et al. (2011) A microprobe for parallel optical and electrical recordings from single neurons in vivo. Nat Methods 8:319–325. 10.1038/nmeth.1572 [PubMed: 21317908]
22. Paxinos G, Franklin KBJ (2013) Paxinos and Franklin's the mouse brain in stereotaxic coordinates Elsevier Academic Press, London
23. Siegel JJ, Taylor W, Gray R et al. (2015) Trace eyeblink conditioning in mice is dependent upon the dorsal medial prefrontal cortex, cerebellum, and amygdala: behavioral characterization and functional circuitry. eNeuro 2:1–29. 10.1523/ENEURO.0051-14.2015
24. Sakamoto T, Endo S (2010) Amygdala, deep cerebellar nuclei and red nucleus contribute to delay eyeblink conditioning in C57BL/6 mice. Eur J Neurosci 32:1537–1551. 10.1111/j.1460-9568.2010.07406.x [PubMed: 20880362]
25. Kehoe EJ, White NE (2002) Extinction revisited: similarities between extinction and reductions in US intensity in classical conditioning of the rabbit's nictitating membrane response. Anim Learn Behav 30:96–111. 10.3758/BF03192912 [PubMed: 12141139]
26. Eccles J, Ito M, Szentágothai J (1967) The cerebellum as a neuronal machine Springer, Heidelberg
27. Miles FA, Fuller JH, Braitman DJ, Dow BM (1980) Long-term adaptive changes in primate vestibuloocular reflex. III. Electrophysiological observations in flocculus of normal monkeys. J Neurophysiol 43:1437–1476 [PubMed: 6768853]
28. Lisberger SG, Fuchs AF (1978) Role of primate flocculus during rapid behavioral modification of vestibuloocular reflex. I. Purkinje cell activity during visually guided horizontal smooth-pursuit eye movements and passive head rotation. J Neurophysiol 41:733–763 [PubMed: 96225]
29. Thach WT (1968) Discharge of Purkinje and cerebellar nuclear neurons during rapidly alternating arm movements in the monkey. J Neurophysiol 31:785–797 [PubMed: 4974877]
30. Ohmae S, Medina JF (2015) Climbing fibers encode a temporal-difference prediction error during cerebellar learning in mice. Nat Neurosci 18:1798–1803. 10.1038/nn.4167 [PubMed: 26551541]
31. Granit R, Phillips CG (1956) Excitatory and inhibitory processes acting upon individual Purkinje cells of the cerebellum in cats. J Physiol 133:520–547 [PubMed: 13368102]
32. Van Dijck G, Van Hulle MM, Heiney SA et al. (2013) Probabilistic identification of cerebellar cortical neurones across species. PLoS One 8:e57669 10.1371/journal.pone.0057669 [PubMed: 23469215]
33. Ruigrok TJH, Hensbroek RA, Simpson JI (2011) Spontaneous activity signatures of morphologically identified interneurons in the vestibulocerebellum. J Neurosci 31:712–724. 10.1523/JNEUROSCI.1959-10.2011 [PubMed: 21228180]
34. Apps R, Hawkes R (2009) Cerebellar cortical organization: a one-map hypothesis. Nat Rev Neurosci 10:670–681. 10.1038/nrn2698 [PubMed: 19693030]

Author Manuscript Author Manuscript Author Manuscript Author Manuscript

35. Garwicz M, Jorntell H, Ekerot CF (1998) Cutaneous receptive fields and topography of mossy fibres and climbing fibres projecting to cat cerebellar C3 zone. J Physiol 512:277–293 [PubMed: 9729638]
36. Mostofi A, Holtzman T, Grout AS et al. (2010) Electrophysiological localization of eyeblink-related microzones in rabbit cerebellar cortex. J Neurosci 30:8920–8934. 10.1523/JNEUROSCI.6117-09.2010 [PubMed: 20592214]
37. Jörntell H, Ekerot CF, Garwicz M, Luo XL (2000) Functional organization of climbing fibre projection to the cerebellar anterior lobe of the rat. J Physiol 522(Pt 2):297–309 [PubMed: 10639105]
38. Uusisaari MY, De Schutter E (2011) The mysterious microcircuitry of the cerebellar nuclei. J Physiol 589:3441–3457. 10.1113/jphysiol.2010.201582 [PubMed: 21521761]
39. Dow RS, Moruzzi G (1958) The physiology and pathology of the cerebellum University of Minnesota Press, Minneapolis, MN
40. Ekerot CF, Jörntell H, Garwicz M (1995) Functional relation between corticonuclear input and movements evoked on microstimulation in cerebellar nucleus interpositus anterior in the cat. Exp Brain Res 106:365–376. 10.1007/BF00231060 [PubMed: 8983981]
41. Hesslow G (1994) Correspondence between climbing fibre input and motor output in eyeblink-related areas in cat cerebellar cortex. J Physiol 476:229–244 [PubMed: 8046640]
42. Kravitz AV, Owen SF, Kreitzer AC (2013) Optogenetic identification of striatal projection neuron subtypes during in vivo recordings. Brain Res 1511:21–32. 10.1016/j.brainres.2012.11.018 [PubMed: 23178332]
43. Smear M, Shusterman R, O'Connor R et al. (2011) Perception of sniff phase in mouse olfaction. Nature 479:397–400. 10.1038/nature10521 [PubMed: 21993623]
44. Lee S-H, Kwan AC, Zhang S et al. (2012) Activation of specific interneurons improves V1 feature selectivity and visual perception. Nature 488:379–383. 10.1038/nature11312 [PubMed: 22878719]
45. Lee KH, Mathews PJ, Reeves AMB et al. (2015) Circuit mechanisms underlying motor memory formation in the cerebellum. Neuron:1–12. 10.1016/j.neuron.2015.03.010
46. Zhao S, Ting JT, Atallah H et al. (2011) Cell type–specific channelrhodopsin-2 transgenic mice for optogenetic dissection of neural circuitry function. Nat Methods 8:745–752. 10.1038/nMeth.1668 [PubMed: 21985008]
47. Kozai TDY, Vazquez AL (2015) Photoelectric artefact from optogenetics and imaging on microelectrodes and bioelectronics: new challenges and opportunities. J Mater Chem B Mater Biol Med 3:4965–4978. 10.1039/C5TB00108K [PubMed: 26167283]
48. Lewicki MS (1998) A review of methods for spike sorting: the detection and classification of neural action potentials. Network 9:R53–R78. 10.1088/0954-898X/9/4/001 [PubMed: 10221571]
49. Rey HG, Pedreira C, Quian Quiroga R (2015) Past, present and future of spike sorting techniques. Brain Res Bull 119:106–117. 10.1016/j.brainresbull.2015.04.007 [PubMed: 25931392]
50. Mauk MD, Ruiz BP (1992) Learning-dependent timing of Pavlovian eyelid responses: differential conditioning using multiple interstimulus intervals. Behav Neurosci 106:666–681 [PubMed: 1503659]
51. Domingo JA, Gruart A, Delgado-García JM (1997) Quantal organization of reflex and conditioned eyelid responses. J Neurophysiol 78:2518–2530 [PubMed: 9356402]
52. Gruart A, Blazquez PM, Delgado-García JM (1995) Kinematics of spontaneous, reflex, and conditioned eyelid movements in the alert cat. J Neurophysiol 74:226–248 [PubMed: 7472326]
53. Powell DA, Churchwell J, Burriss L (2005) Medial prefrontal lesions and Pavlovian eyeblink and heart rate conditioning: effects of partial reinforcement on delay and trace conditioning in rabbits (Oryctolagus Cuniculus). Behav Neurosci 119:180–189. 10.1037/0735-7044.119.1.180 [PubMed: 15727523]

Author Manuscript Author Manuscript Author Manuscript Author Manuscript

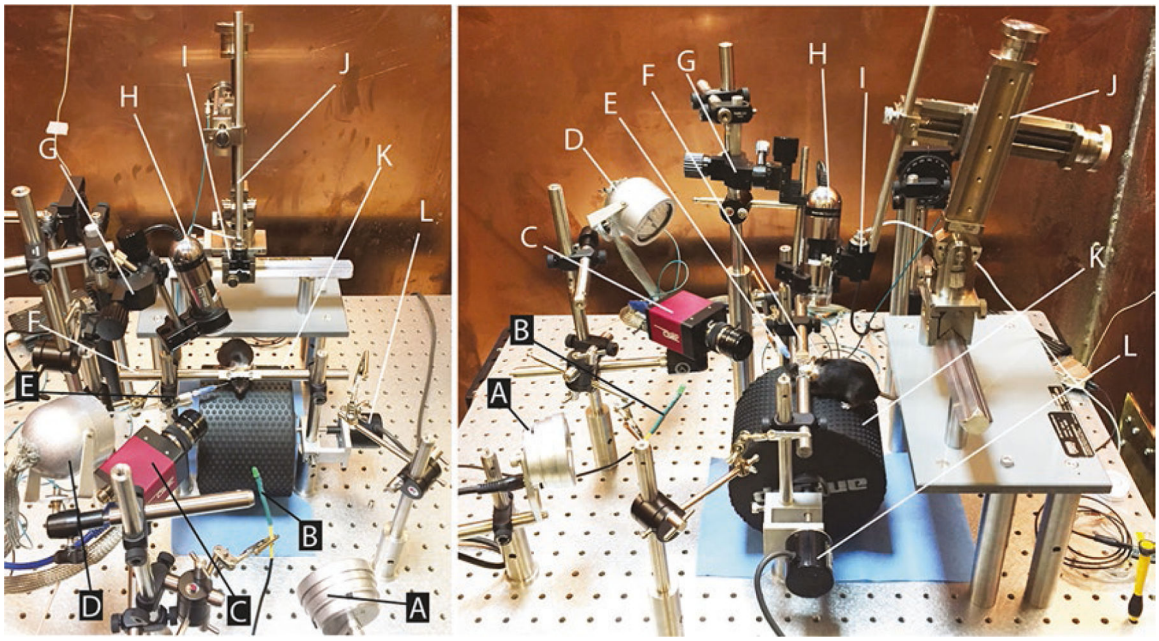

Fig. 1.

Apparatus for head-fixed electrophysiology, optogenetics, and behavior experiments. The two photographs show a top view (*left*) and side view (*right*) of the assembled components. Aluminum foil electrical shields have been removed from equipment (e.g., infrared light (**d**)) for better visibility of materials. Labels reference components described in the materials section. Briefly: (**a**) Multi-Field Magnetic Speakers (TDT MF1). (**b**) BNC to LED cable (custom). (**c**) High-speed camera (AVT GE680). (**d**) Infrared light (Towallmark Crazy Cart 48-LED IR Infrared Night Vision Illuminator). (**e**) Blunt needle (23G), adapter (WPI 13160), and tubing for delivering air puff (Clippard URH1–0402-CLT). (**f**) Bars for holding headplate (custom). (**g**) Three-axis micromanipulator (Narishige UMC3). (**h**) Handheld microscope camera (Dino-Lite AD-4013 MTL). (**i**) One-axis micromanipulator (Narishige MMO-220A modified to remove ball joint). (**j**) Stereotaxic micromanipulator (Narishige SMM-100 with custom shaft (EDMS16–054b) and modified MA-2 micromanipulator stand (SDMS16–033a)). (**k**) Treadmill (custom). (**l**) Rotary encoder (Karlsson Robotics E6C2-CWZ3E 1024 count/revolution quadrature encoder)

Author Manuscript Author Manuscript Author Manuscript Author Manuscript

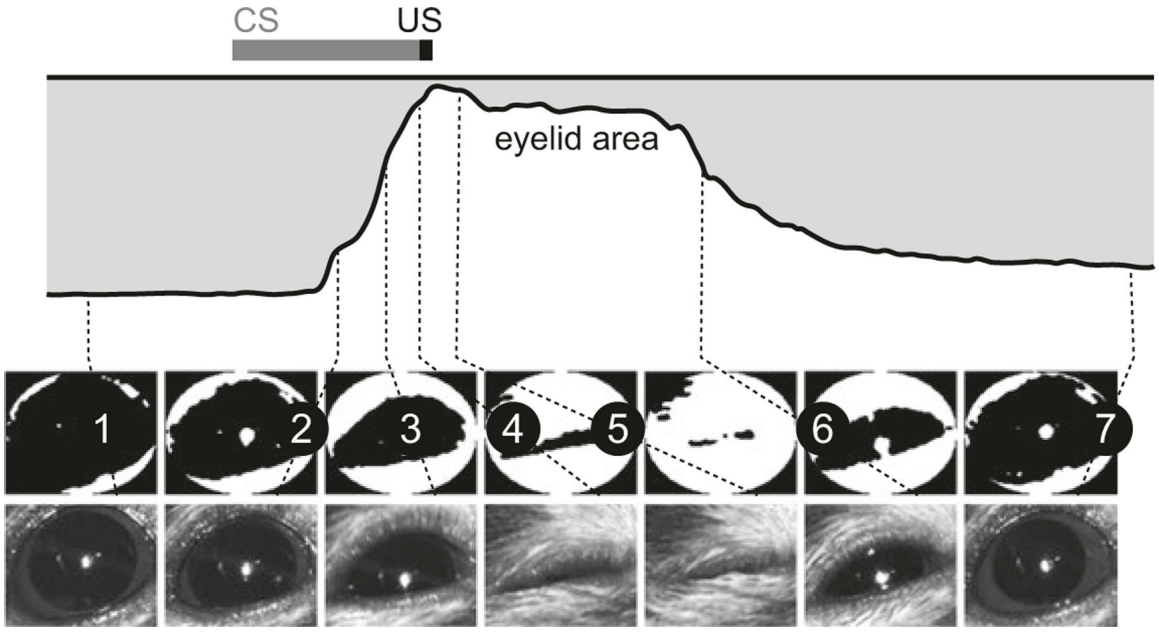

Fig. 2.

Eyelid movement detection algorithm. Illustration of algorithm used to measure eyelid closure using FEC. Key time points during a paired CS-US trial are indicated by numbered lines connecting video frames to the corresponding points in the eyelid traces. Used with permission from [12]

Author Manuscript Author Manuscript Author Manuscript Author Manuscript

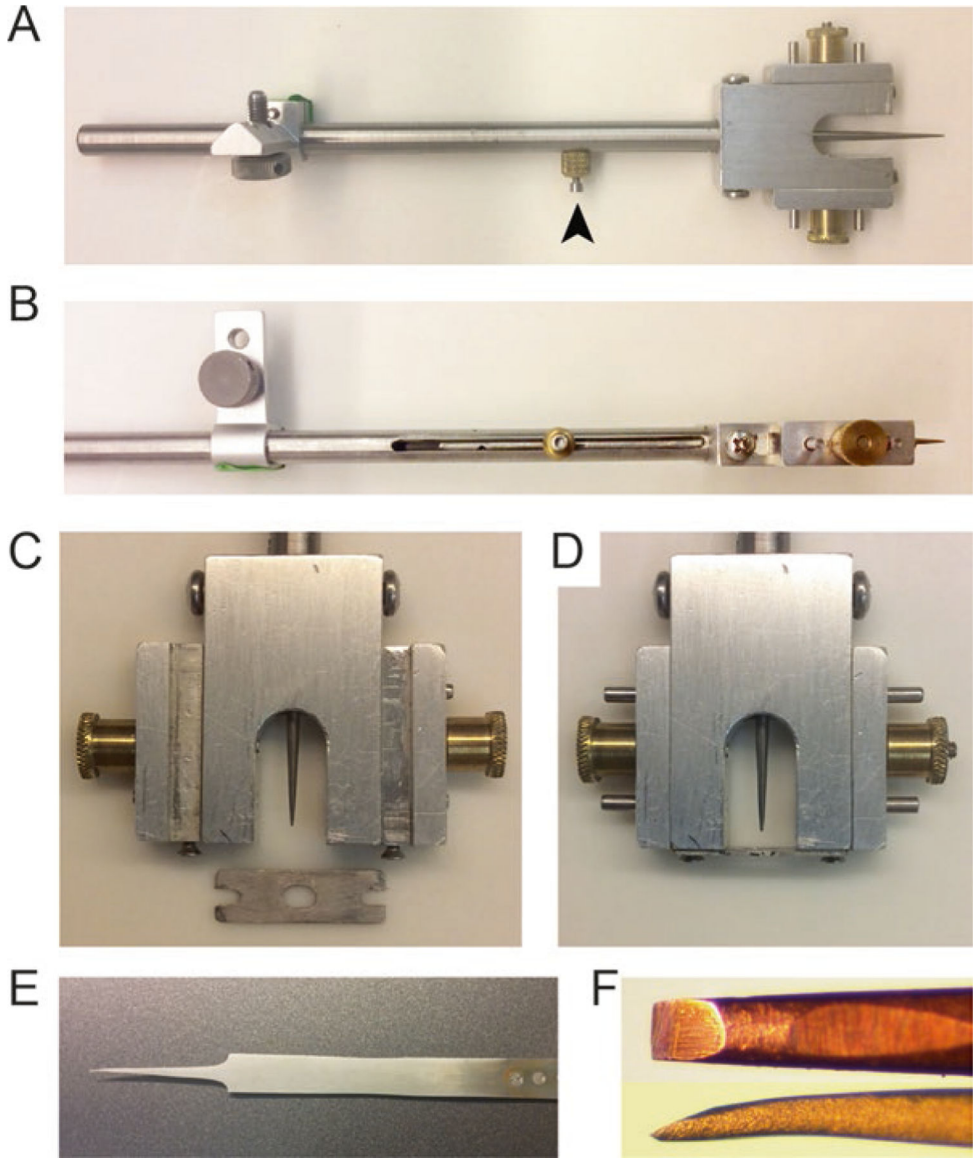

Fig. 3.

Surgery tools. (**a**–**d**) A custom-made head plate holder that can be mounted on the stereotaxic manipulator arm. The stylus is retractable and can be held by the stopper screw (*arrow head*). Zoomed-in view of the holder before (**c**) and after (**d**) holding the headplate. The headplate is held between the horizontally moving screws. (**e**, **f)** A hand made dura cleaning tool. The tool was made by splitting the arms of FST forceps and sharpening the tip (**f**) by fine grit polishing paper

Author Manuscript Author Manuscript Author Manuscript Author Manuscript

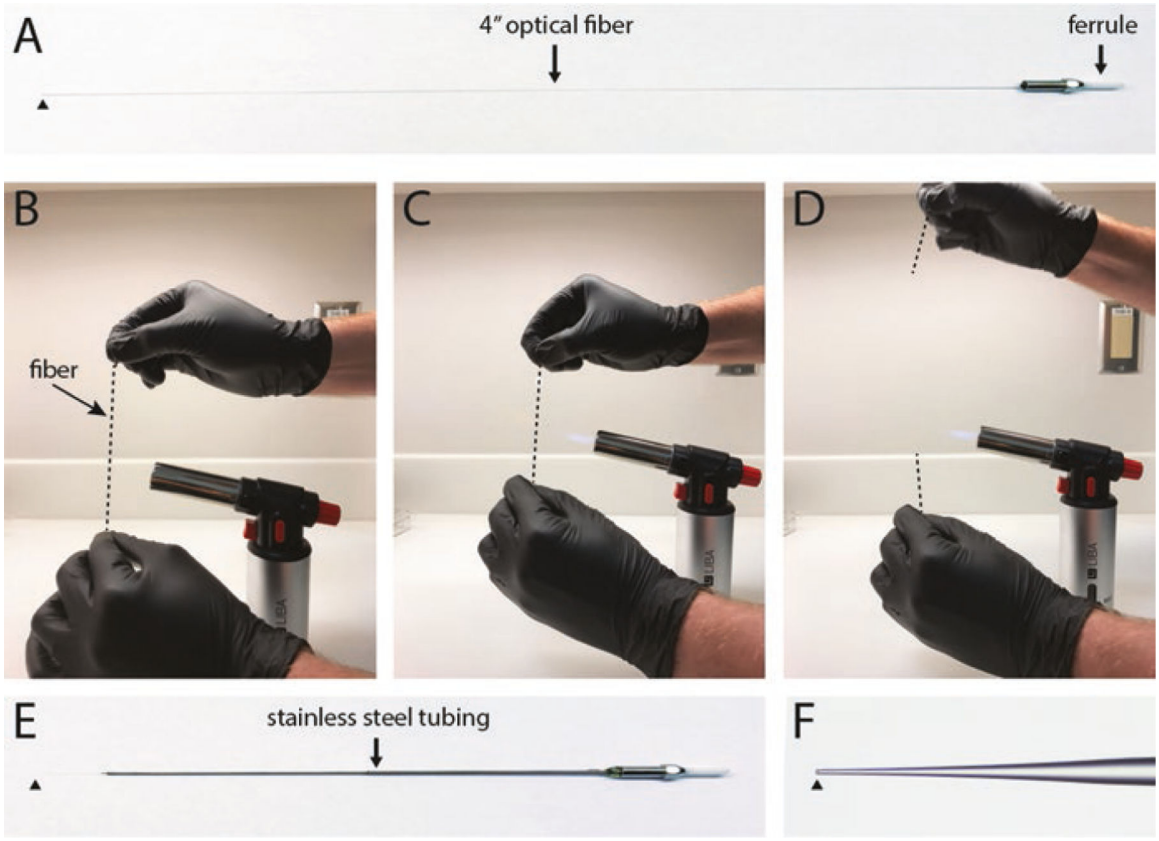

Fig. 4.

Pulling optical fibers for acute photostimulation. Start with an approximately 4” connectorized fiber (**a**). Gently heat the fiber around its midpoint over a butane flame, and pull the two ends in opposite directions to stretch the glass and reduce the diameter (**b**–**d**). Secure the shaft of the pulled fiber in stainless steel tubing using cyanoacrylate glue (**e**). Cleave the fiber tip to desired diameter (**f**). Black arrowheads indicate location of fiber tip

Author Manuscript Author Manuscript Author Manuscript Author Manuscript

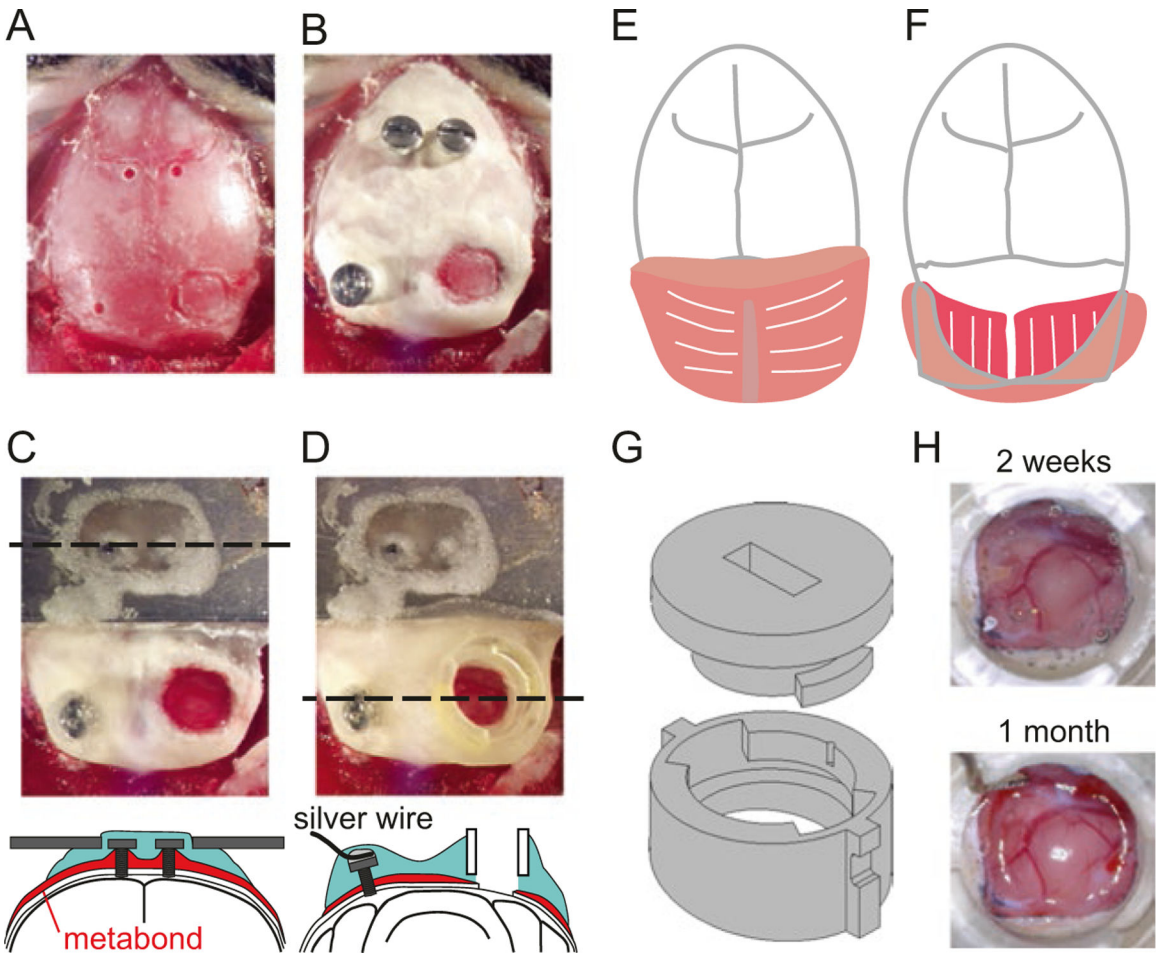

Fig. 5.

Headplate and craniotomy surgery. (**a**–**d**) View of mouse's skull after drilling screw holes and marking the outline for craniotomy (**a**), after implanting screws and covering the skull with dental cement (**b**), after securing the headplate and craniotomy (**c**), and after securing the recording chamber (**d**). Coronal schematic view is shown at the level of dashed line in (**c**) and (**d**). (**e**) The first layer of the occipital muscle (the splenius capitis) is cut in the midline and detached from the occipital bone. (**f**) The second layer of the occipital muscle (the splenius trapezius) is seen under the folded first layer. The second layer is also detached from the occipital bone (not shown) so that the skull surrounding the craniotomy can be covered by dental cement. (**g**) Technical drawing of 3D printed recording chamber and interlocking lid. Lid is locked in place by inserting it into grooves of chamber and turning 45° clockwise using a small flathead screwdriver. (**h**) Healthy dura 2 weeks (*top*) and 1 month (*bottom*) after the craniotomy surgery

Author Manuscript Author Manuscript Author Manuscript Author Manuscript

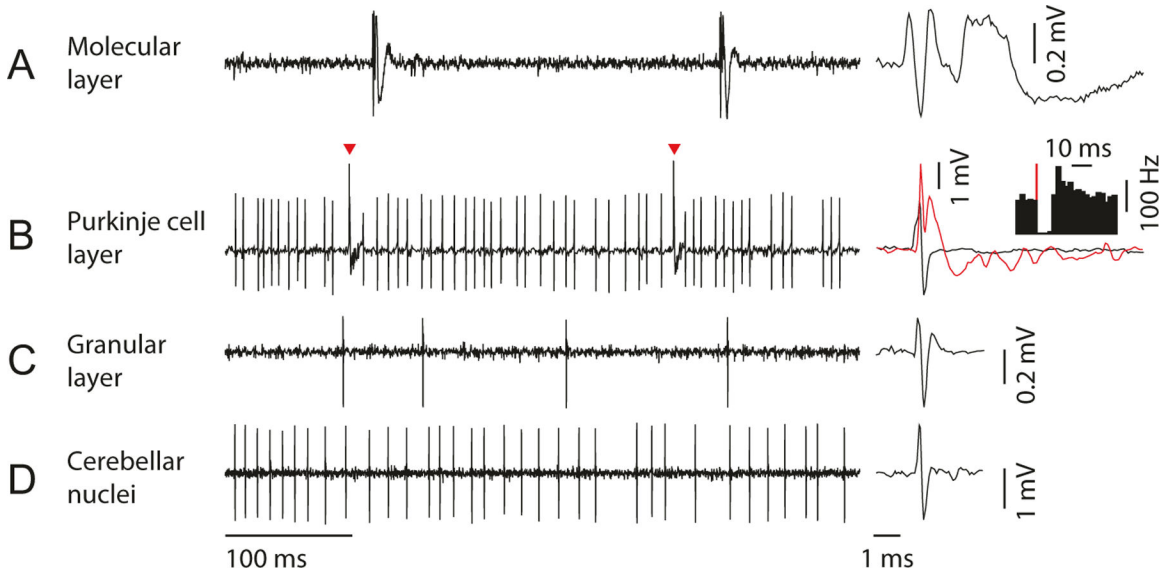

Fig. 6.

Neural activity patterns in each layer of cerebellar cortex and deep cerebellar nuclei. (**a**) In molecular layer, complex spike from Purkinje cell dendrite can be isolated. Zoomed-in view of complex spike waveform (*right*) shows long tail with spikelets, which can be detected as a low-frequency sound in audio monitor. (**b**) In Purkinje cell layer, simple spike and complex spike (*red arrowhead and red trace*) can be simultaneously isolated. Simple spike firing (y-axis of the inset histogram is firing rate) pauses for 10–30 ms after each complex spike (*red line*). (**c**) In granular layer, a low firing rate cell (putative Golgi cell) can be isolated. Complex spikes should not be detectable in this layer. (**d**) In deep cerebellar nuclei, cells with high spontaneous firing rate are often isolated (putative excitatory projection neuron). The cerebellar nuclei should be separated from the cerebellar cortex by white matter (which lacks prominent spiking activity and sounds quiet on the audio monitor)

Author Manuscript Author Manuscript Author Manuscript Author Manuscript

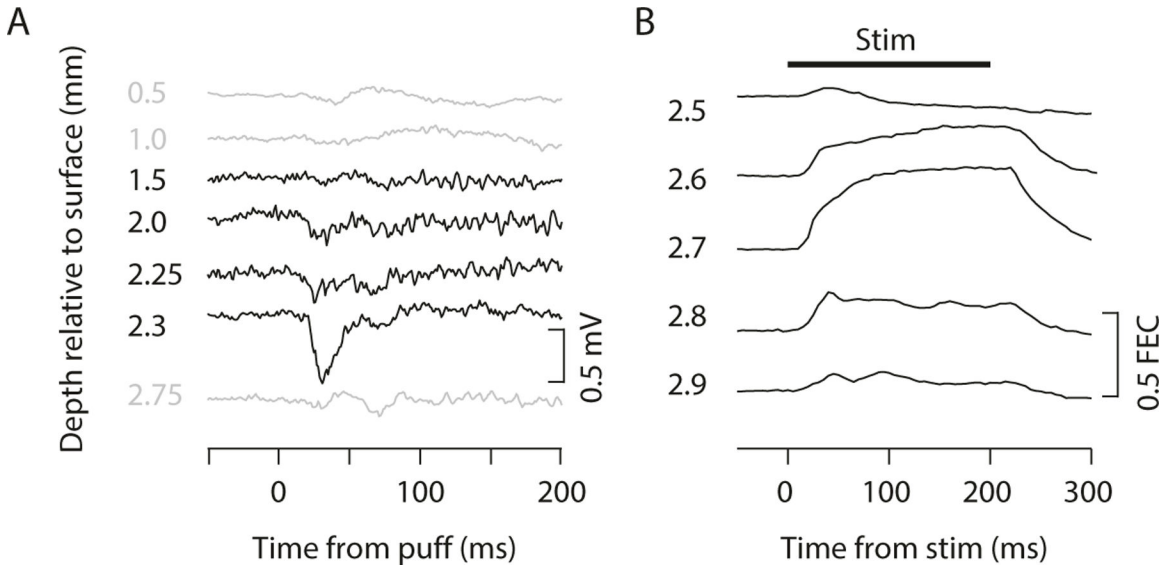

Fig. 7.

Functional mapping of cerebellar cortex and nuclei. (**a**) LFP recordings at different depths through cerebellar cortex during periocular stimulation (air puff). Region with periocular climbing fiber receptive fields is indicated by large negative deflection in LFP signal following air puff to eye. (**b**) Eyelid traces during microstimulation at different depths through DCN. The eyeblink region of DCN is indicated by the location at which microstimulation at currents less than approximately 10 μA produces large and reliable eyelid closure that is sustained for the duration of the stimulation (indicated by *black line at top*). Used with permission from [12]

Author Manuscript Author Manuscript Author Manuscript Author Manuscript

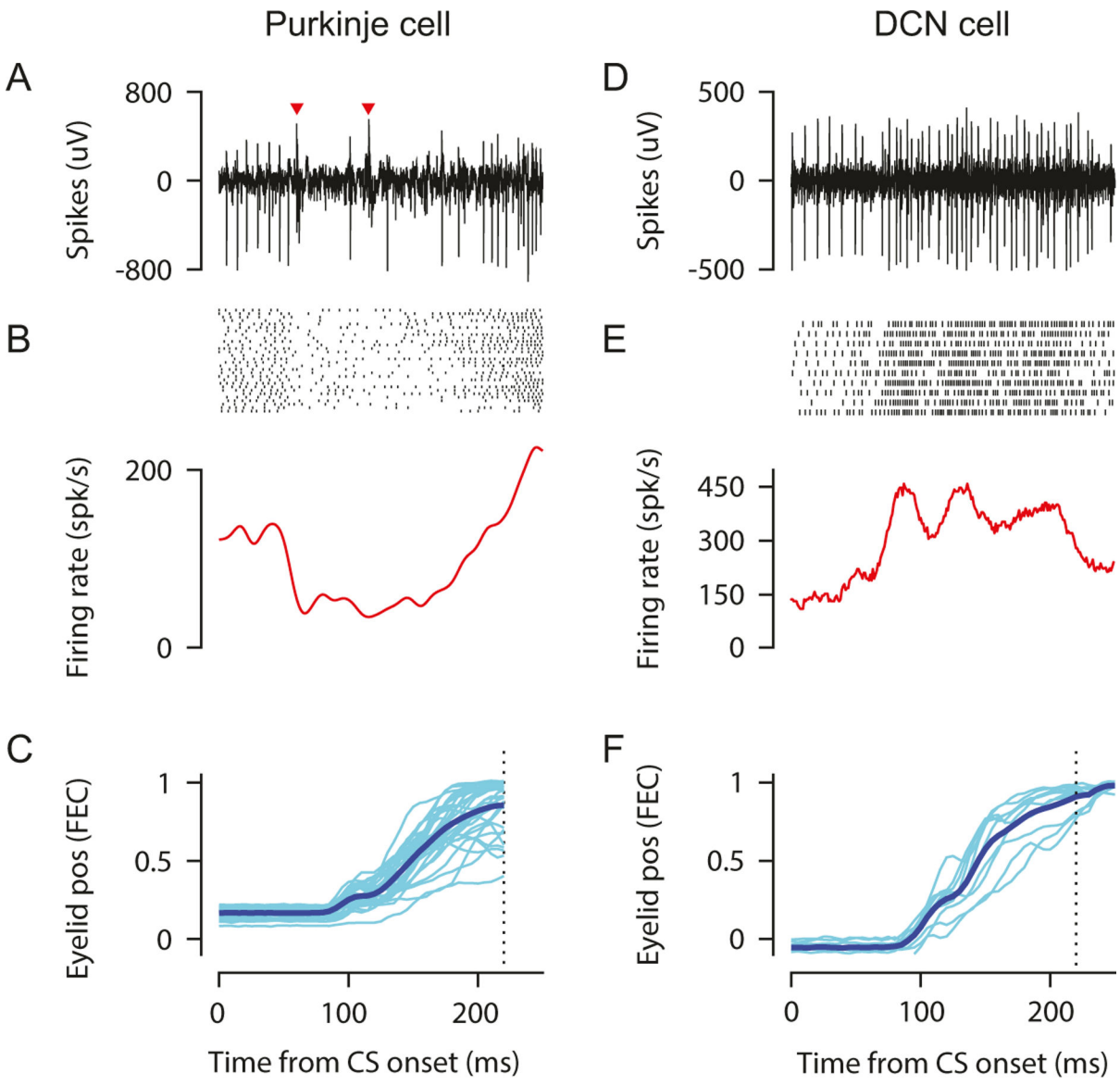

Fig. 8.

Example Purkinje (**a–c**) and DCN (**d–f**) cell recorded in eyeblink hot spots of cerebellar cortex and anterior interpositus during EBC. (**a**, **d**) Extracellular signal during a single trial; (**b**, **e**) raster of spike times (*top*) and peristimulus time histogram (*bottom*) for multiple paired trials; (**c**, **f**) eyelid positions for the same trials (*light thin traces*). Average eyelid position trace indicated by dark thick trace. Used with permission from [12]